

Material Systems for Blast-Energy Dissipation

IMPLAST 2010

Benjamin Langhorst
Corey Cook
James Schondel
Henry S. Chu

October 2010

The INL is a
U.S. Department of Energy
National Laboratory
operated by
Battelle Energy Alliance



This is a preprint of a paper intended for publication in a journal or proceedings. Since changes may be made before publication, this preprint should not be cited or reproduced without permission of the author. This document was prepared as an account of work sponsored by an agency of the United States Government. Neither the United States Government nor any agency thereof, or any of their employees, makes any warranty, expressed or implied, or assumes any legal liability or responsibility for any third party's use, or the results of such use, of any information, apparatus, product or process disclosed in this report, or represents that its use by such third party would not infringe privately owned rights. The views expressed in this paper are not necessarily those of the United States Government or the sponsoring agency.

Material Systems for Blast-Energy Dissipation

Dr. Benjamin Langhorst^{a*}, Corey Cook^{a,b}, James Schondel^a, Dr. Henry S. Chu^a

^a Armor and Explosive Materials and Technologies, Idaho National Laboratory, Idaho Falls, ID, USA

^b Montana Tech, The University of Montana, Butte, MT, USA

* Corresponding author: WCB Mailstop 3214, PO Box 1625, Idaho Falls, ID 83415.
Benjamin.Langhorst@inl.gov Phone: (208) 526-6756

ABSTRACT

Lightweight panels have been designed to protect buildings and vehicles from blast pressures by activating energy dissipation mechanisms under the influence of blast loading. Panels were fabricated which featured a variety of granular materials and hydraulic dissipative deformation mechanisms and the test articles were subjected to full-scale blast loading. The force time-histories transmitted by each technology were measured by a novel method that utilized inexpensive custom-designed force sensors. The array of tests revealed that granular materials can effectively dissipate blast energy if they are employed in a way that they easily crush and rearrange. Similarly, hydraulic dissipation can effectively dissipate energy if the panel features a high fraction of porosity and the panel encasement features low compressive stiffness.

1. Introduction

To keep pace with protection levels provided by ballistic armor research, energy-dissipative armor materials and systems must be advanced to protect buildings and vehicles from explosive overpressures. Blast energy dissipation can be achieved by activating one or more energy “sinks” within a protective panel (e.g. kinetic, thermal, strain, sound, potential energies) [1,2]. The elastic storage and release of strain energy that can be achieved by many simple monolithic material systems alters the time history of blast loads that the system transmits, but does not dissipate the total transmitted impulse.

This study explored several lightweight, inexpensive, energy-absorbing materials and systems that could be employed to dissipate the blast loads transmitted to an underlying structure or vehicle. Solid materials rapidly conduct shock waves through the protective panel without dissipating energy. To avoid such behavior, novel technologies were designed that featured soft layers with high fractions of porosity that permit crushing. Various designs of these material systems were manufactured and subjected to blast loads and their transmitted force-time histories were measured by custom sensors.

Impulse is defined as the time integral of a force-time history and is analogous to, but not equivalent to, energy. In section 2 (Methods), energy is discussed rather than impulse because of the focus on energy dissipation mechanisms featured by the blast mitigation material systems. However, as testing is explained and data is presented, impulse will be discussed rather than energy, because it is more quantifiable as it enters and exits a protective panel.

2. Methods

2.1. Materials

2.1.1. Granular-filled panels

Pumice is a natural earthen material derived from solidified volcanic lava and can be found all around the world. It forms when volcanic gasses agglomerate into various-sized bubbles that cannot escape the liquid magma

matrix before solidification. The presence of trapped bubbles makes pumice very porous and consequently lightweight (density: $\rho \sim 0.6 - 0.8$ g/cc). Pumice can be mined, ground, and filtered into a wide range of granule sizes. Additionally, because of its accessibility in mines, its natural abundance, and simple post-processing techniques, pumice is a relatively inexpensive armor material. Pumice granules feature relatively low strengths and can be crushed into a fine powder, dissipating energy through the creation of new surfaces.

Perlite is another porous granular material that results from volcanic activity. Like pumice, it can be easily mined, but one additional post-mining step gives perlite a significantly lower density than pumice (dry perlite density: $\rho \sim 0.2 - 0.3$ g/cc). Natural perlite contains a lot of moisture trapped in its pores. When the moist granules are flash heated, the trapped water vapor escapes the pores by breaking granules apart – similar to popcorn popping. The resulting granules, called perlite, are approximately one third the density of pumice that has been slowly and completely dried and feature slightly lower compressive strengths in this study. Pumice and perlite were utilized in a variety of cladding system designs, each of which is described below.

Each design group sought to employ the granular material as an energy dissipative material by holding it in place until the arrival of the incoming blast wave, and then allowing it to crush and crumble under the applied blast pressure, dissipating energy as it moved and deformed. Prior testing demonstrated that complete confinement of the pumice by surrounding it with a rigid matrix is ineffective. Specifically, panels were fabricated by submerging 50 vol% of pumice in a solid epoxy matrix. Under low blast levels with an impulse less than 500 psi-msec (3.45 MPa-msec) no deformation was visible and under very high blast levels, the panels fractured mostly within the epoxy matrix and failed to activate the intended granular deformation and dissipation mechanisms. Consequently, the panels designed for this series of testing each featured different methods of granular binding.

2.1.1.a. Stiff contact binder

Dry granules were mixed with a small fraction of epoxy to lightly coat the surfaces of each particle. Then the coated particles were poured into a box with dimensions approximately 12 inch X 12 inch X 1.25 inch (305 mm X 305 mm X 31.75 mm). As the epoxy cured, the granular matrix was bound together by epoxy adhesion between adjacent contacting particles. Three of these panels were fabricated: one that featured pumice bound together by a solid epoxy surface coating, one that featured pumice bound together by an expanding epoxy surface coating (the epoxy accepts air and slightly expands during the curing process), and one that featured perlite bound together by a solid epoxy surface coating. The pumice-filled panels featured ~75 wt. % pumice and the remainder was epoxy. The perlite-filled panel featured ~20 wt. % perlite and the remainder was epoxy.

2.1.1.b. Soft contact binder

An alternative binding approach was explored using aerosol adhesive instead of epoxy. Dry granules were poured into a flat, square box with dimensions approximately 12 inch X 12 inch X 1.25 inch (305 mm X 305 mm X 31.75 mm). As dry granules were poured into the box, spray adhesive was applied and the partially-coated granules were mixed to promote thru-thickness adhesion and eliminate the laminar features inherent to this processing method. This manufacturing technique resulted in a spongy matrix in which adjacent granules were loosely bound to each other. One panel was fabricated with pumice by the method described above. A second panel was fabricated with pumice by the method described above with exception of the panel's central core which was not sprayed with adhesive in an effort to leave a loose core in the center of the panel. The pumice-filled panels featured ~90 wt. % pumice and the remainder was epoxy. The perlite-filled panel featured ~30 wt. % perlite and the remainder was epoxy.

2.1.1.c. Contained granules

The final granular-filled technology featured loose granular material contained in a soft foam pocket. The pocket was made of slow-recovery polyurethane foam chosen for its hysteretic dissipative properties. The foam was 0.25 inches (6.4 mm) thick and the foam's compliance ensured that pressure would be applied evenly across the entire granular face, and not to a mere few high-sitting granules. During testing, the panels were hung vertically, causing the granules to slightly sag in their pocket. The sag was not significant enough to be detrimental to performance, and in practice the sag could be mitigated by decreasing the size of each pocket to the point where the maximum amount of sag is acceptable.

2.1.2. Hydraulic-dissipative panels

A second category of dissipative panels featured hydrogel (sodium-doped polyacrylate powder) suspended in a sandwich panel core which featured pores that allowed constricted flow between adjacent compartments within

the panel. Fiberglass hexagonal honeycomb cores were constructed into different configurations to investigate the effectiveness of energy dissipation by constricted hydraulic flow. The hexagonal prism honeycomb core cells measured approximately 0.375 inches (9.5 mm) from flat to flat. The fiberglass honeycomb walls were made of a woven mesh with inter-weave pores that were approximately 0.06 inches (1.5 mm) square and large enough to permit hydraulic flow. In order to prevent hydraulic flow prior to the application of blast pressure, water was suspended in a hydrogel state. The viscous gel was incapable of short-term cell wall penetration but, upon application of pressure, the gel released the suspended water. The water and some viscous gel then penetrated the cell walls and flowed as directed by applied pressure and gravity.

A series of four panels were fabricated, each with solid polyethylene front and back faces that were 0.125 inches (3.2 mm) and 0.25 inches (6.4 mm) thick respectively, and flexible side walls to allow thru-thickness panel compression. Each of the four panels featured a different core design.

The first featured a 1.5 inch (38.1 mm) thick honeycomb core oriented with its soft direction facing the blast in order to encourage panel compression. Approximately 50% of its volume was filled with pre-saturated hydrogel. The second panel featured the same 1.5 inch (38.1 mm) thick honeycomb core, oriented with its soft direction facing the blast, but it contained no hydrogel – i.e. the honeycomb was empty. The third and fourth panels featured “bi-layer” designs with hydrogel in the layer closest to the incoming blast front and a porous membrane between the layers to allow hydraulic flow between the layers as the panel was crushed. Pores in the membrane were approximately 0.025 inch (0.64 mm) squares. The third panel featured a 0.5 inch (12.7 mm) thick empty (no hydrogel fill) honeycomb back layer oriented with its soft direction facing the blast, and a 1.0 inch (25.4 mm) thick 50%-hydrogel-filled honeycomb front layer also oriented with its soft direction facing the blast. The fourth panel explored a different back layer design: 0.5 inch (12.7 mm) thick empty honeycomb oriented with its stiff direction facing the blast, and a 1.0 inch (25.4 mm) thick 50%-hydrogel-filled honeycomb front layer, oriented with its soft direction facing the blast.

These four designs explored the effects of hydrogel inclusion, multi-layer designs, and stiff-versus-soft back layers. The hydrogel was pre-saturated with water at a ratio of 1:50 by weight. The panels were tested within one week of their fabrication and were still wet at the time of testing.





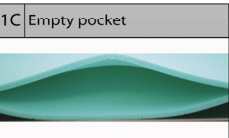

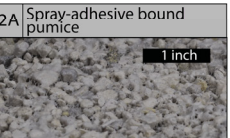

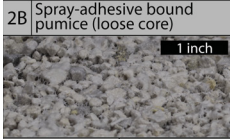
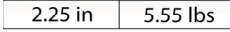
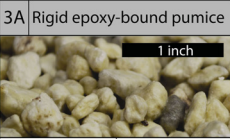

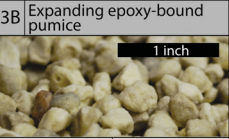

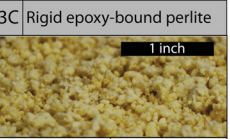
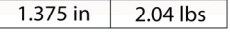
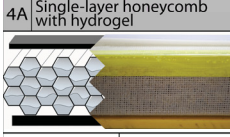

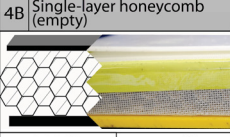

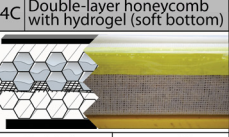

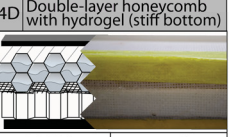

| ID | | Name / Description | |
|----------|---|---|---|
| | | Photo of Panel | |
| | | Thickness | Weight |
| 1A | Pumice-filled pocket |  |  |
| 2.25 in | 3.57 lbs | | |
| 1B | Perlite-filled pocket |  |  |
| 2.50 in | 1.78 lbs | | |
| 1C | Empty pocket |  |  |
| 0.75 in | 1.17 lbs | | |
| 2A | Spray-adhesive bound pumice |  |  |
| 1.875 in | 5.09 lbs | | |
| 2B | Spray-adhesive bound pumice (loose core) |  |  |
| 2.25 in | 5.55 lbs | | |
| 3A | Rigid epoxy-bound pumice |  |  |
| 1.50 in | 4.66 lbs | | |
| 3B | Expanding epoxy-bound pumice |  |  |
| 1.375 in | 4.22 lbs | | |
| 3C | Rigid epoxy-bound perlite |  |  |
| 1.375 in | 2.04 lbs | | |
| 4A | Single-layer honeycomb with hydrogel |  |  |
| 2.00 in | 4.50 lbs | | |
| 4B | Single-layer honeycomb (empty) |  |  |
| 1.75 in | 2.68 lbs | | |
| 4C | Double-layer honeycomb with hydrogel (soft bottom) |  |  |
| 2.00 in | 3.83 lbs | | |
| 4D | Double-layer honeycomb with hydrogel (stiff bottom) |  |  |
| 1.75 in | 4.26 lbs | | |

Figure 1 – Twelve different protective material systems were constructed and tested. They are presented here along with pre-testing thicknesses and weights. All panels measured 12 inch X 12inch (.3 m X .3 m) in frontal area and were attached to a 0.25 inch (6.4 mm) thick rigid polyethylene back face. Panels 4A, 4B, 4C, and 4D also featured a 0.125 inch (3.2 mm) thick rigid polyethylene front face.

2.2. *Physical Test Setup*

A unique test setup was designed to measure panel response to applied blast pressures. Three test sleds were positioned side-by-side, each capable of holding two panels at a centerline height of 36 inches (0.9 meters) above the ground. Because the test articles were too numerous to be tested simultaneously, they were divided into test groups and a series of blasts was conducted. To provide a consistent basis on which to judge panel performance, one of the six test article slots was used to hold a baseline panel during each blast. The baseline panel was a 0.25 inch (6.4 mm) thick sheet of solid polyethylene.

The sled faces were each fitted with a 1 inch (25.4 mm) thick “back plate” made of ultra-high molecular weight polyethylene (UHMWPE) that covered the entire 24 inch X 24 inch (0.6m X 0.6m) square area of the sled faces. The polyethylene back plates were used to constrain the test panels and corresponding transmitted force sensors as depicted in Figure 2.

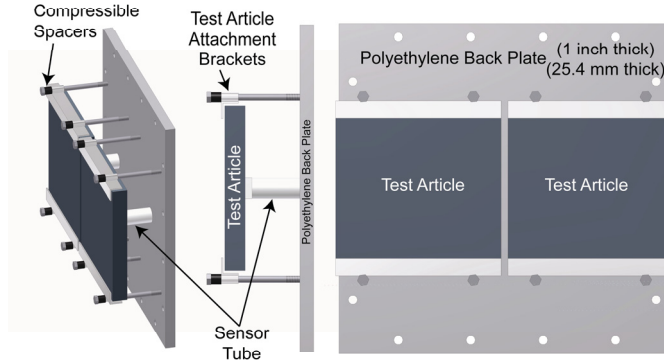


Figure 2 – Test Article Mounting Scheme. Two test panels were mounted on each sled by the attachment scheme shown here. The polyethylene back plate was bolted directly to the steel sled face.

To create the explosions, 175 lbs. (79.4 kg) of ANFO was mixed at a ratio of 6 parts ammonium nitrate to 1 part fuel oil and was placed in a cardboard drum that measured 18.5 inches (0.47m) in diameter and 36 inches (0.9m) tall. To ensure a center-primed detonation, a C-4 booster was placed in the geometric center of the ANFO charge. To prevent sympathetic detonation of the ANFO by the detonation cord, a piece of thin-walled, clear plastic tubing with a length of 18 inches (0.46 m) and a diameter of 1.25 inches (32 mm) was wrapped around the detonation cord, conducting and isolating it through the ANFO to the C-4 booster. The entire test setup is shown in Figure 3.

Table 1 – Details of bomb components including TNT equivalent. (RE = relative efficiency)

| Charge construction | | |
|--|-----------|---------------------------|
| Component | RE Factor | TNT Equivalent |
| 175 lbs ammonium-nitrate and fuel oil (ANFO) | 0.86 | 150.5 lbs (68.3kg) |
| 2.25 lbs M112 block C-4 | 1.37 | 3.08 lbs (1.4kg) |
| 3 feet of 50 grain det. cord | 1.27 | 0.027 lbs (12.2g) |
| 20 grams deta-prime booster | 1.27 | 0.0558 lbs (25.3g) |
| 1 blasting cap (Detonator) | 1.00 | 0.0033 lbs (1.4g) |
| Total Net Equivalent Weight TNT: | | 153.6 lbs (69.7kg) |

Table 2 – Predicted bomb behavior at 50 feet (15.2m) standoff distance. From ConWep [3]. (N.E.W. = net equivalent weight)

| ConWep-predicted blast performance at 50 feet using total N.E.W. TNT 153.6 lbs and hemispherical configuration | |
|---|---------------------------------|
| Time of arrival | 21.0 msec |
| Peak incident pressure | 10.9 psi (75.2 MPa) |
| Peak reflected pressure | 28.2 psi (194.4 MPa) |
| Reflected impulse | 105 psi-msec (724 MPa-msec) |
| Shock front velocity | 1430 feet / sec (435.8 m / sec) |

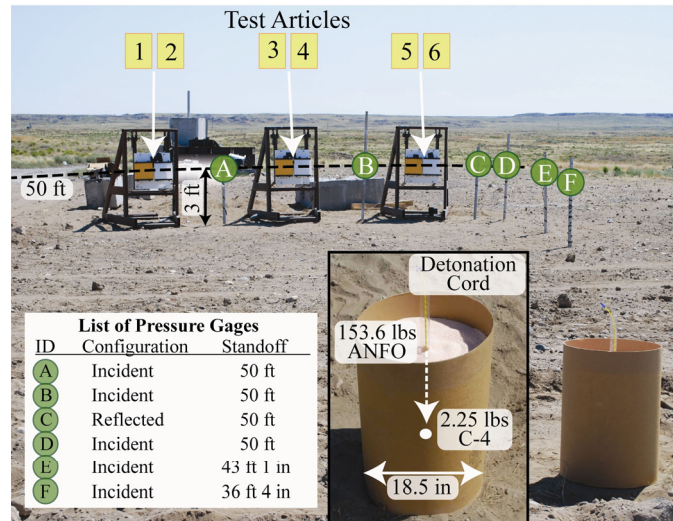


Figure 3 – Blast-test setup. The entire test layout included up to six test articles (labeled 1-6) simultaneously mounted on each of three test sleds, six free-field pressure gages (labeled A-F) and a bomb.

2.3. Instrumentation Setup

A 16-channel data acquisition system (meDAQ by HiTechniques) was used to record dynamic measurements. Pressure transducers were arranged around the test sled setup in order to measure incident and reflected overpressure at various standoff distances. Additionally, transmitted force-time history was measured behind each panel using custom-designed load cells [4]. This sensor design, inspired by the Hopkinson Pressure Bar [5-7] featured many advantages over commercially available sensor solutions. The sensors were manufactured with low cost, off-the-shelf materials and were optimized for sensitivity at the range of predicted blast loads, which was less than 2000 lbs (907kg). Additionally, they were piezo-resistive in nature, which permitted the controlling data acquisition computer to be located hundreds of yards away from the blast without requiring the use of inline signal amplifiers. Polycarbonate tubes were instrumented with full Wheatstone-bridge strain gage setups and located behind the test articles to measure the dynamic loads transmitted by the panels. The completed transmitted force sensors were capable of reliably measuring the peak blast loads imparted by testing, but were also sensitive enough to discern load differences of one pound (0.45 kg) in an indoor laboratory setting.

High-speed photography was also acquired to enable coupled visual-numerical analysis. Three Phantom high speed cameras were used to observe deformation from different angles.

3. Results

3.1. Blasting consistency

The series of four blasts generated very consistent pressure-time histories. The incident pressure-time histories of all four blasts are compared in Figure 4 along with the corresponding impulse-time histories calculated by integrating the pressure-time histories. Incident pressure was measured at locations in the vicinity of the test

articles to ensure that the four different groups of test articles were subjected to very similar blast loads. The locations of the measurements presented in Figure 4 are shown in Figure 3 as pressure gage IDs B and D.

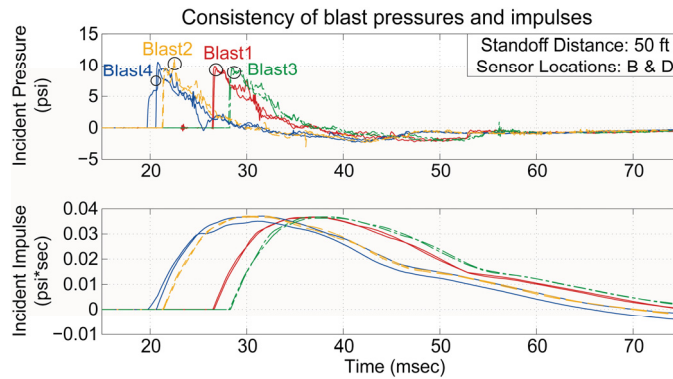


Figure 4 – Incident pressure-time histories measured at pressure-gage locations B and D noted in Figure 3 (50 feet standoff) for all four blasts.

3.2. Measured force-time histories

The force-time histories transmitted by each test article are presented in Figure 5. These measurements were acquired by the strain-gaged sensor tubes as described in section 2.3. Along with each force-time history, the transmitted impulse-time history (integral of force-time history) is concurrently plotted.

Table 3 presents tabulated performance statistics for each test article. Peak load reduction and impulse reduction values were calculated using data from the first 3.3 msec after blast wave arrival. Reduction values were calculated by comparing the performance (e.g. peak transmitted load, or transmitted impulse) of each test article to the baseline panel with which it was tested.

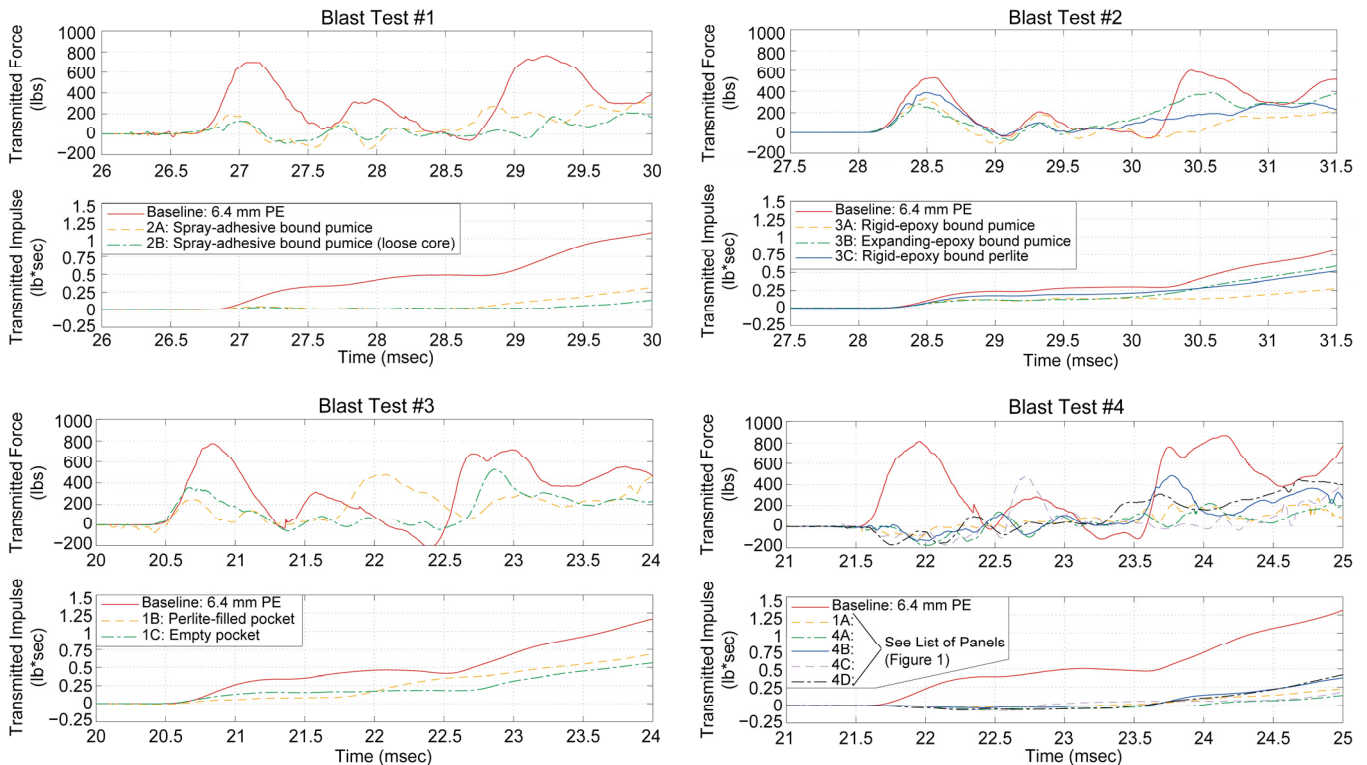


Figure 5 – Transmitted force- and impulse-time histories for panels tested in four consecutive blast tests.

Table 3 – Performance statistics presented for each of the twelve panels tested.

| | | | PERFORMANCE STATISTICS | |
|----------|---|-----------|------------------------|-------------------|
| Panel ID | Description | Blast No. | Peak Load Reduction | Impulse Reduction |
| 1A | Pumice-filled pocket | 4 | -66% | -84% |
| 1B | Perlite-filled pocket | 3 | -37% | -42% |
| 1C | Empty pocket | 3 | -32% | -52% |
| 2A | Spray-adhesive bound pumice | 1 | -56% | -72% |
| 2B | Spray-adhesive bound pumice (loose core) | 1 | -66% | -88% |
| 3A | Rigid epoxy-bound pumice | 2 | -7% | -66% |
| 3B | Expanding epoxy-bound pumice | 2 | -37% | -28% |
| 3C | Rigid epoxy-bound perlite | 2 | -32% | -36% |
| 4A | Single-layer honeycomb with hydrogel | 4 | -54% | -92% |
| 4B | Single-layer honeycomb (empty) | 4 | -38% | -74% |
| 4C | Double-layer honeycomb with hydrogel (soft bottom) | 4 | -43% | -90% |
| 4D | Double-layer honeycomb with hydrogel (stiff bottom) | 4 | -37% | -72% |

4. Discussion

4.1. Bomb consistency

The series of four bombs performed very consistently. Figure 4 shows the incident pressure-time histories recorded at points B and D (located as shown in Figure 3). Each blast created peak incident pressures at the 50 foot (15.2 m) standoff distance of ~10 psi (~69 MPa), and incident impulses of ~37 psi-msec (~255 MPa-msec). The bomb consistency provides a repeatable loading history to which each panel was subjected.

The time axes on Figure 5 were shortened to highlight the first 3-4 msec after the blast arrival. This enhances features in the short time frame and cuts misleading features in the late-time regime (e.g. panels bouncing out of alignment and resting unevenly on the sensors). After 3 msec, the applied pressure had dissipated to 50% of its peak, and two-thirds of the impulse had been applied. At later times, panels bounce and slightly rearrange, imparting small loads on the sensors that have negligible effects on structural survivability, but affect the measured impulse values when maintained for longer time periods.

4.2. Granular-filled panels

The granular-filled panels (panel series 1, 2 and 3 in Figure 1) reduced the impulse by 28-88%, with the best performance exhibited by spray-adhesive bound pumice. In addition to exhibiting superior performance, granular-filled technologies are both weight- and cost-effective. The use of plentiful and natural earthen materials makes the technologies inexpensive and the low density of pumice and perlite makes the technology lightweight – both important factors in the protection of buildings and vehicles. As a general trend, performance was enhanced in designs that enabled greater granular mobility. These results pertain to granular material that originated in southeast Idaho, and material from other origins has not yet been quantified.

4.3. Hydrogel panels

The honeycomb-core panels demonstrated an interesting phenomenon: the delay of blast load transmission by more than 1 msec. In fact, the measured transmitted loads were initially negative – a phenomenon which has not yet been explained. While the authors cannot yet positively attribute this negative phase, they can dispel a few possible causes. Preliminary analyses suggest that this measurement is (1) not an artifact of an internal shock wave pressurizing the air inside the hollow sensor tube, (2) not caused by reflected shock waves within the sensor tube wall, and (3) not caused by uneven front face loading and consequential sensor tube bending. In addition, a tensile load could not be imparted by the test articles on their sensors as no connections existed between their contacting surfaces. One possible explanation that remains is the wrap-around of the blast wave into the sensor cavity behind the test articles. It is possible that the transmitted load in the first millisecond was so

small that its resulting signal was dominated by blast effects on the outer walls of the sensor. The designs examined in this study will likely behave differently when subjected to blast waves with different characteristics. Optimized systems for given blast characteristics will likely be functions of multiple design variables including pore size and fluid viscosity.

5. Conclusions

Granular materials are a weight- and cost-effective means of blast energy dissipation – if they are employed appropriately. Individual granules must be mobilized to enable rearrangement, crumbling, and crushing, but also contained to prevent the introduction of a secondary debris hazard.

Honeycomb structures significantly modified the transmitted force time histories and ultimately reduced the total transmitted impulse. The inclusion of hydrogel and the activation of constricted hydraulic flow dissipated more energy and enhanced the effectiveness of the blast-mitigation panels.

However, questions remain regarding the source of the negative transmitted force measurements and further blast testing is necessary to investigate the effect of blast wave wrap-around. Future testing should feature shielding that isolates the sensor cavity from the blast environment.

6. Acknowledgements

This work was funded by laboratory-directed research and development funds from Idaho National Laboratory (FY 2009 – NS161-“Development and Evaluation of Low Pressure Energy Absorbing Materials and Methods for Buildings”). Pumice samples were provided by Hess Pumice Products (Malad, ID), and Patz Materials and Technologies (Benicia, CA) assisted in the fabrication of the fiberglass honeycomb cores and the epoxy-bound granular cores. Gregory Clemens (Idaho National Laboratory) provided valuable mentoring and insight into innovative testing and instrumentation approaches.

7. References

- [1] Dawson, M.A., G.H. McKinley, L.J. Gibson. (2009) “The dynamic compressive response of an open-cell foam impregnated with a non-newtonian fluid.” *J. App. Mech.***76**. pp.061011
- [2] Sabiri, N.E., Montillet, A. and Comiti, J. (1997) “Pressure drops of non-newtonian purely viscous fluid flow through synthetic foams.” *Chem. Eng. Comm*, **156**: 1, pp.59-74.
- [3] ConWep [computer software]. (1997) (Version 2.1.0.8). USAE Engineer Research and Development Center, Vicksburg, MS.
- [4] Langhorst, B.R., C. Cook, J. Schondel, H.S. Chu. (2010) “Measurement of transmitted blast force-time histories.” *Sens Imaging*, **11**:51-60.
- [5] Hopkinson, B. (1914) “A method of measuring the pressure produced in the detonation of high explosives or by the impact of bullets.” *Phil. Trans. R. Soc.* **A213**. pp.437.
- [6] Kolsky, H. (1949) “An Investigation of the Mechanical Properties of Materials at very High Rates of Loading.” *Proc. Phys. Soc.***B62**. pp.676-700.
- [7] Lindholm, U.S. (1964) “Some experiments with the split Hopkinson pressure bar.” *J. Mech. Phys. Solids* **12**. pp.317-335.